Roughness Induced Backscattering in Optical Silicon Waveguides

Francesco Morichetti*
Policom—DEI, Politecnico di Milano, Via Colombo 81, 20133 Milano, Italy
and Fondazione Politecnico di Milano, Via Garofalo 39, Milano 20133, Italy

Antonio Canciamilla, Carlo Ferrari, Matteo Torregiani, Andrea Melloni, and Mario Martinelli
Policom—DEI, Politecnico di Milano, Via Colombo 81, 20133 Milano, Italy
(Received 29 June 2009; revised manuscript received 13 November 2009; published 20 January 2010)

We report on the direct observation of backscattering induced by sidewall roughness in high-index-contrast optical waveguides based on total internal reflection. Our results demonstrate that backscattering is one of the most severe limiting factors in state-of-the art silicon on insulator nanowires employed in densely integrated photonics. We also derive the general relationship between backscattering and geometrical and optical parameters of the waveguide. Further, the role of roughness in polarization rotation and coupling with higher-order modes is pointed out.

DOI: 10.1103/PhysRevLett.104.033902 PACS numbers: 42.25.Fx, 42.81.Dp, 42.82.Et

Although propagation in optical waveguides affected by random wall perturbations has been intensively studied since the origin of integrated optics [1], in recent years interest in this topic has experienced a dramatic rebirth. The reason is that, in high-index-contrast (HIC) waveguides employed in densely integrated photonics [2], surface imperfections are the main source of propagation loss and scattering [3,4]. A widespread example is provided by waveguides in silicon on insulator (SOI) technology, with state-of-the-art propagation losses of 1 dB/cm [5], almost 2 orders of magnitude higher than in the best low-index-contrast waveguides [6].

In addition to radiation loss, sidewall roughness is also expected to cause backward coupling with counterpropagating guided modes [7]. Recent studies have pointed out the problem in photonic crystal (PhC) waveguides, where backscattering loss, scaling quadratically with the waveguide group index [8–11], represents the ultimate limit to devices operating in slow light regime. Surprisingly, backscattering in HIC optical waveguides has not received as much attention as radiation loss has, even though it can originate a variety of impairments in optical systems, such as fading noise, intersymbol interference, transfer function distortion, crosstalk, and return loss degradations. The main aim of this Letter is to show how dramatically the problem of backscattering emerges in HIC waveguides based on total internal reflection (TIR). Our results reveal that a few hundreds of micrometers long single mode SOI waveguide with a loss of only a few dB/cm induces a backscattering that can hinder its exploitation in many practical applications. Further, we also show how sidewall roughness induced backscattering is related to geometrical and optical parameters of the waveguide, polarization rotation effects, and coupling with higher-order modes.

The complex amplitude of backscattering was measured by using an advanced measurement technique. According to Fig. 1, the intensity and the phase of backscattering are extracted from the interference between the field r_e reflected at the air-waveguide external interface and the spatial distribution $h_r(z)$ of field backscattered along the waveguide. From the power spectral density (PSD) of the overall reflected field, the complex autocorrelation $R(z)$ of the space (time) domain response is derived by inverse Fourier transformation. Figure 1 shows a typical $R(z)$ versus the normalized longitudinal coordinate z/L_w, L_w being the waveguide physical length. The central peak of the autocorrelation $R(0)$ gives the total reflected power, that is typically dominated by the external power reflection $|r_e|^2$. An ideally infinite number of replicas $R(m)$ are generated at m integer waveguide lengths by multiple round-trips inside the waveguide. The spatial distribution of the waveguide complex backscattering $h_r(z)$ can be extracted from the distributed signal in the space interval $0 < z/L_w < 1$, being the interferometric term

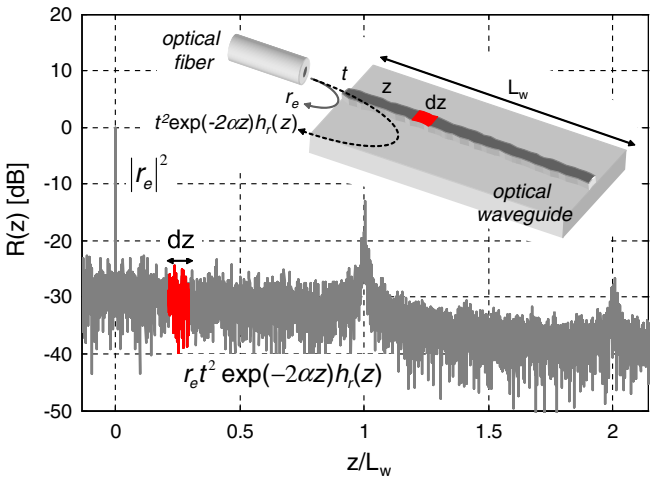

FIG. 1 (color online). Autocorrelation $R(z)$ of the optical field reflected by a waveguide with reflective end facets. A schematic of the measurement technique is shown in the inset.

$r_e t^2 \exp(-2\alpha z) h_r(z)$, where t is the field fiber-to-waveguide coupling coefficient and α is the field propagation loss. Parameters α and r_e are estimated directly from $R(z)$, while t can be measured by a conventional cutback loss characterization. Note that, for a z-invariant structure like a straight waveguide with a constant cross section, the backscattering $\langle h_r(z) \rangle$ averaged over a generic waveguide section dz does not depend on z.

The described technique was employed to measure backscattering in HIC optical waveguides fabricated in SOI technology. The waveguides have a rectangular silicon core (refractive index $n_{\mathrm{Si}} = 3.45$) with a height of 220 nm and width w, and are buried in SiO_2 ($n_{\mathrm{SiO_2}} = 1.45$). The refractive index contrast of the waveguides is 140%. Surface roughness of the silicon core sidewalls has a standard deviation of about 2 nm and a correlation length of about 60 nm. All the measurements were performed at telecom wavelengths (1.55 μm) by using lensed optical fibers to couple light into the waveguides and extracting the reflected field by means of a circulator.

Figure 2(a) shows the measured propagation loss (averaged over a 60 nm wavelength range around 1550 nm) of waveguides with different width w for transverse electric (TE, circles) and transverse magnetic (TM, diamonds) input polarization. With the exception of waveguides with $w = 230$ nm and $w = 700$ nm, whose behavior is extensively discussed in the remainder of the Letter, TE polarization experiences a higher propagation loss than TM polarization because of its higher sensitivity to sidewall roughness. At the cutoff of the first higher-order mode ($w = 500$ nm), the fundamental TE and TM modes exhibit a loss of 2.4 and 1.1 dB/cm, respectively. The backscattering of the same waveguides is shown in Fig. 2(b) for TE (circles) and TM (diamonds) input polarization. The figure shows the backscattering PSD, averaged over a 60-nm wavelength range, for a waveguide length of 1 mm. In agreement with theoretical predictions [4], the higher TE sensitivity to sidewall roughness results in a higher backscattering level, the difference between the two polarizations increasing from about 10 dB in larger waveguides ($w = 600$ nm) to about 20 dB in narrower waveguides ($w = 300$ nm).

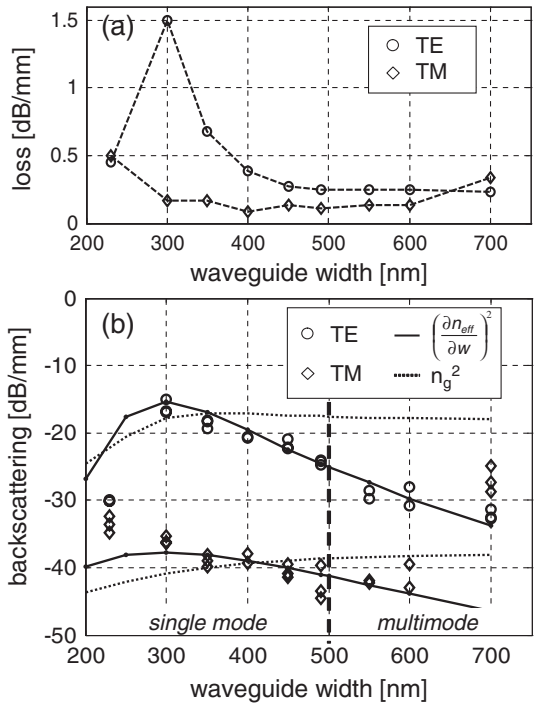

FIG. 2. Measured (a) propagation loss and (b) backscattering of SOI waveguides versus w for TE (circles) and TM (diamonds) input polarization. Measurements are averaged over the wavelength range 1520–1580 nm. In (b), experimental data of three sets of waveguides are numerically fitted with Eq. (1) (solid line) and with a n_g^2 curve (dotted line).

The comparison between Figs. 2(a) and 2(b) points out that backscattering gives only a small contribution (<10%) to the overall propagation loss α, which is largely dominated by radiation loss, as theoretically predicted in [4]. To give some numbers, backscattering is responsible for only 0.015 dB/mm loss in a 490-nm-wide waveguide ($\alpha = 0.25$ dB/mm) and less than 0.15 dB/mm loss for $w = 300$ nm ($\alpha = 1.5$ dB/mm). Nonetheless, if in silicon photonics a loss of a few dB/cm is acceptable in most applications, backscattering emerges as a severe limiting factor for two main reasons. First, specifications on the acceptable return loss of typical devices for optical communication are difficult to fulfill. A 200 μm long classical single mode waveguide ($w = 490$ nm) exhibits for TE polarization a backscattering level as high as -32 dB. As a comparison, the same back reflection is produced by a 1-m-long low-index-contrast waveguide [6] and by Rayleigh backscattering in an infinitely long standard optical fiber. Further, considering the 300-nm-wide waveguide it turns out that for a length of 8 mm the transmitted power becomes equal to the backscattering, both roughly equal to 5% of the input power. Second, if the waveguide is employed to realize resonant structures such as ring resonators, backscattering is coherently enhanced according to the square of the finesse of the resonator and causes strong transfer function distortions [12].

The results shown in Fig. 2 allow us to clarify how backscattering depends on the geometrical and optical waveguide parameters. By using a perturbative model that takes into account the change of mode field distribution with w, we found that backscattering in TIR waveguides depends on waveguide mode effective index n_{eff} through the square of its partial derivative with respect to w. The numerical fit of the measured data with a curve $(\partial n_{\mathrm{eff}}/\partial w)^2$ [solid lines in Fig. 2(b)] holds for both polarizations and for any measured waveguide, with the exception of the narrowest ($w = 230$ nm) and the widest ($w = 700$ nm) ones, whose deviation is justified later on. The full explanation of the theoretical model is out of the scope of this work and will be illustrated in detail in future contributions, but a simple intuitive explanation can be

provided here. Waveguide roughness can be considered as a spatial superposition of random sinusoidal perturbations, i.e., Bragg gratings [7]. In the small perturbation regime, a single sinusoidal corrugation of amplitude δw produces at the Bragg wavelength λ_B a field back reflection $H_r(\lambda_B) = \kappa dz$, where

$$\kappa = \frac{\pi}{\lambda_B}\delta n_{\text{eff}} = \frac{\pi}{\lambda_B}\frac{\partial n_{\text{eff}}}{\partial w}\delta w \tag{1}$$

is the grating coupling coefficient and δn_{eff} is the waveguide effective index perturbation. Equation (1) is valid for every waveguide shape and index contrast and states that, given a corrugation depth δw, the backscattered power depends only on $\partial n_{\text{eff}}/\partial w$ squared. It is worth observing that this derivative is maximum when the mode field width is minimum, i.e., when the confinement is maximum [$w =$ 300 nm in Fig. 2(b)]. This critical dimension should be avoided to reduce waveguide backscattering. Simple derivations show that in the case of slab waveguides the equality $(\partial n_{\text{eff}}/\partial w)\delta w = (n_g - n_{\text{eff}})/w$ holds rigorously and backscattering is related to $(n_g - n_{\text{eff}})^2$ only, with n_g the waveguide group index.

The dotted curves in Fig. 2(b) show the numerical fit of the experimental data with a $n_g^2(w)$ dependence, this behavior being predicted [8,9] and observed [10] in several recent works on PhC waveguides. It is evident that in TIR waveguides there is no direct relationship between backscattering and n_g. This result is not surprising, because the change of w not only makes n_g change, but it also modifies the mode field distribution and its interaction with sidewall roughness. Therefore, in TIR waveguides a universal relationship between n_g and backscattering is likely to be inconsistent.

The discrepancy from the theoretical model of waveguides $w = 230$ nm and $w = 700$ nm is now explained by analyzing the state of polarization (SOP) of the transmitted field. Figure 3 shows the SOP evolution on the Poincaré sphere in the wavelength range between 1550 and 1562 nm at the output of waveguides with $L_w = 5.7$ mm and $w =$ 230, 490, and 700 nm, respectively. In the 490-nm-wide waveguide, the input TE polarization is mapped at the output around the $-S_1$ point of the sphere [3(b1)], while the input TM polarization is mapped onto the orthogonal $+S_1$ point [3(b2)], RCP being the right circular polarization state. Data cluster dispersion is due to the limited extinction ratio (about 20 dB) of the polarization controller placed before the launch fiber. At the waveguide output the polarization extinction ratio degrades (improves) to about 15 dB (25 dB) in the case of input TE (TM) polarization, because of a combined effect of waveguide polarization dependent loss (1 dB), different fiber-to-waveguide coupling t (9 dB/facet for TE, 6 dB/facet TM), and different Fabry-Pérot fringes depth (4 dB for TE, 1.5 dB for TM). The 230-nm-wide waveguide exhibits a dramatically different behavior [Figs. 3(a1) and 3(a2)]. In the wavelength range, the output SOP wraps around the sphere

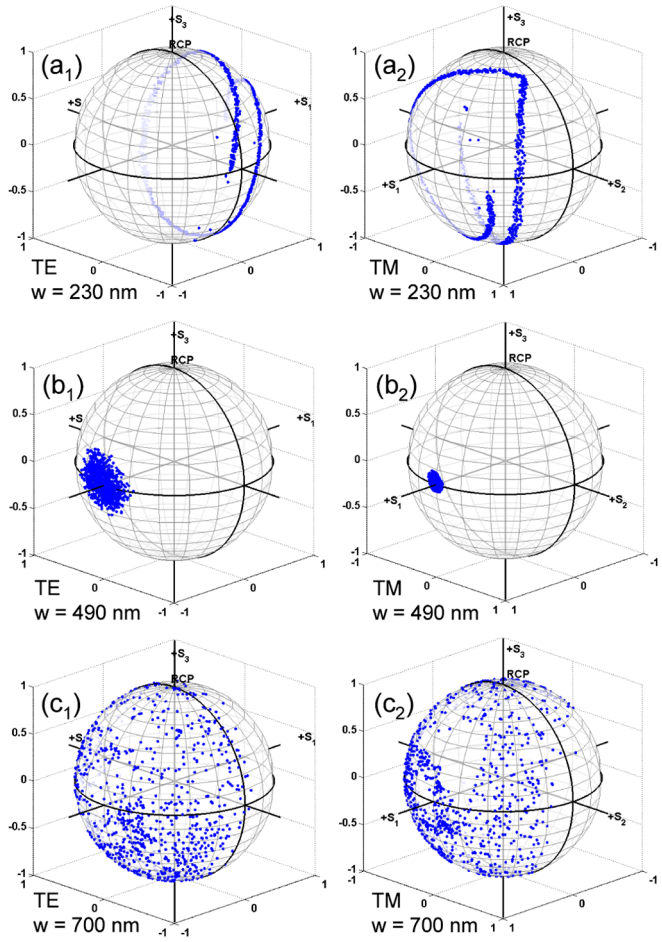

FIG. 3 (color online). Evolution of the SOP over a 12 nm wavelength range at the output of 5.7-mm-long SOI waveguides with different widths w: (a) $w = 230$ nm, (b) $w = 490$ nm, (c) $w = 700$ nm.

due to a strong polarization rotation induced by sidewall roughness along the waveguide. This happens because the nearly square waveguide supports quasidegenerate TE and TM modes ($n_{\text{eff,TE}} = 1.522$, $n_{\text{eff,TM}} = 1.519$), thus making polarization coupling efficiently phase matched. The wavelength periodicity of the process $\Delta\lambda_{\text{SOP}} = \lambda^2/(\Delta n_g L_w) = 9$ nm depends on the inverse relative group index of the two modes ($\Delta n_g = n_{g,\text{TE}} - n_{g,\text{TM}} = 0.033$). Because of such a strong polarization coupling, the waveguide exhibits the same average backscattering and loss for TE and TM input polarization, as shown in Fig. 2. Likewise, the high TM backscattering of the 700-nm waveguide is associated with a polarization coupling mechanism since it is pretty well phase matched with the first higher-order TE_1 mode ($n_{\text{eff,TE}_1} = 1.875$, $n_{\text{eff,TM}} = 1.959$). As shown in Figs. 3(c1) and 3(c2) the SOP evolution is much faster than in Figs. 3(a1) and 3(a2) because the wavelength periodicity is $\Delta\lambda_{\text{SOP}} = 620$ pm ($\Delta n_g = 0.472$). As the backscattering coefficient $(\partial n_{\text{eff}}/\partial w)^2$ of the higher-order TE_1 mode is a factor of 5 greater than that of the fundamental TE mode, a strong backscattering is

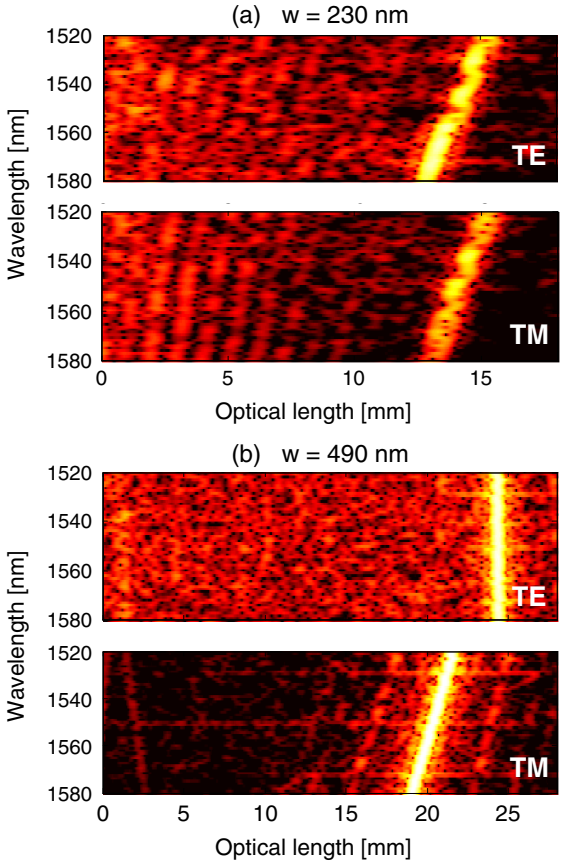

FIG. 4 (color online). Space-wavelength distribution of back reflection along 5.7-mm-long SOI waveguides (a) in the presence ($w = 230$) or (b) in the absence ($w = 490$) of polarization coupling.

observed when the fundamental TM mode is launched into the 700-nm-wide waveguide, clarifying the result shown in Fig. 2(b).

From the measurement of the phase of the complex backscattering, it is possible to observe where, along the waveguide, backscattering is produced. Figure 4 shows in a map the spatial distribution of backscattering along two waveguides. Each row λ_i of the maps is obtained by inverse Fourier transforming a 3-nm-wide Gaussian-shaped subband of the backscattering PSD centered at λ_i. The lighter color in the map is associated with higher back reflection. The waveguide input is at the left-hand boundary of the map, while the bright line at the right-hand side corresponds to the output facet reflection, whose position on the optical length axis depends on the group index dispersion. Figure 4(b) shows that in the 490-nm-wide waveguide the TE mode has a higher group index than the TM mode ($n_{g,\mathrm{TE}} = 4.19$ and $n_{g,\mathrm{TM}} = 3.69$ at 1550 nm), a lower group index dispersion ($dn_{g,\mathrm{TE}}/d\lambda = 2.9 \times 10^{-4}$ nm^{-1}, $dn_{g,\mathrm{TM}}/d\lambda = 6.5 \times 10^{-3}$ nm^{-1}), and a higher backscattering, with a noiselike texture along the waveguide. In the 230-nm-wide waveguide of Fig. 4(a) polarization coupling makes the TE and TM distribution almost identical, with the same group index ($n_{g,\mathrm{TE}} = n_{g,\mathrm{TM}} = 2.46$) and dispersion ($dn_{g,\mathrm{TE}}/d\lambda = 6.7 \times 10^{-3}$ nm^{-1}). Because of polarization coupling, in this waveguide backscattering exhibits a periodic pattern with a period $L_B = \lambda/(n_{\mathrm{eff,TE}} - n_{\mathrm{eff,TM}}) = 450$ μm visible on the SOP evolution along the waveguide [13], the local maxima (minima) occurring when polarization is prevalently TE (TM).

In conclusion, sidewall roughness induced backscattering in silicon HIC optical waveguides has been studied and measured experimentally. We demonstrate that backscattering in typical SOI waveguides (1) is at least 3 orders of magnitude higher than in low-index-contrast waveguides, (2) depends on the sensitivity of the mode effective index on the waveguide cross-sectional size and cannot be simply related to n_g, and (3) is much weaker for TM polarization than for TE, provided that no polarization coupling occurs along the waveguide. These results reveal that state-of-the art silicon photonic waveguides (and more generally high-index-contrast waveguides) exhibit back reflection levels that can prevent their use in many practical applications and that the TM polarization could be the viable strategy to mitigate the impairment. The comparison with backscattering in PhCs [14] and coupled resonator optical waveguides [12] is left to future specific contributions.

This work was partially supported by the European Project SPLASH (6th FP).

*morichetti@elet.polimi.it

[1] D. Marcuse, Bell Syst. Tech. J. **48**, 3187 (1969).
[2] B. Jalali and S. Fathpour, J. Lightwave Technol. **24**, 4600 (2006).
[3] K. K. Lee, D. R. Lim, L. C. Kimerling, J. Shin, and F. Cerrina, Opt. Lett. **26**, 1888 (2001).
[4] C. G. Poulton, C. Koos, M. Fujii, A. Pfrang, T. Schimmel, J. Leuthold, and W. Freude, IEEE J. Sel. Top. Quantum Electron. **12**, 1306 (2006).
[5] M. Gnan, S. Thoms, D. S. Macintyre, R. M. De La Rue, and M. Sorel, Electron. Lett. **44**, 115 (2008).
[6] K. Takada and S. Mitachi, J. Lightwave Technol. **16**, 639 (1998).
[7] F. Ladouceur and L. Poladian, Opt. Lett. **21**, 1833 (1996).
[8] S. Hughes, L. Ramunno, Jeff F. Young, and J. E. Sipe, Phys. Rev. Lett. **94**, 033903 (2005).
[9] S. G. Johnson, M. L. Povinelli, M. Soljacic, A. Karalis, S. Jacobs, and J. D. Joannopoulos, Appl. Phys. B **81**, 283 (2005).
[10] R. J. P. Engelen, D. Mori, T. Baba, and L. Kuipers, Phys. Rev. Lett. **101**, 103901 (2008).
[11] M. Patterson, S. Hughes, S. Combrie, N. V.-Quynh, A. De Rossi, R. Gabet, and Y. Jaouen, Phys. Rev. Lett. **102**, 253903 (2009).
[12] F. Morichetti *et al.*, "Coherent Backscattering in Optical Microring Resonators" (to be published).
[13] A. Melloni and F. Morichetti, Phys. Rev. Lett. **98**, 173902 (2007).
[14] B. Wang, S. Mazoyer, J. P. Hugonin, and P. Lalanne, Phys. Rev. B **78**, 245108 (2008).